



Device simulation of inverted $\text{CH}_3\text{NH}_3\text{PbI}_{3-x}\text{Cl}_x$ perovskite solar cells based on PCBM electron transport layer and NiO hole transport layer

Peng Zhao, Ziyi Liu, Zhenhua Lin*, Dazheng Chen, Jie Su, Chunfu Zhang*, Jincheng Zhang, Jingjing Chang*, Yue Hao

State Key Laboratory of Wide Band Gap Semiconductor Technology, Shaanxi Joint Key Laboratory of Graphene, School of Microelectronics, Xidian University, 2 South Taibai Road, Xi'an 710071, China



ARTICLE INFO

Keywords:

Perovskite solar cells
Device simulation
NiO
PCBM

ABSTRACT

The perovskite solar cells have attracted great attention owing to their low cost and high performance. For perovskite solar cells, metal oxides demonstrated great potential with much higher charge carrier mobility and superior stability than organic materials. In this study, we employed NiO as hole transport layer and chloride-doped $\text{CH}_3\text{NH}_3\text{PbI}_3$ ($\text{CH}_3\text{NH}_3\text{PbI}_{3-x}\text{Cl}_x$) as absorber due to its enhanced performance. We investigated the effects of several parameters on the solar cell performance through device simulation. It was found that solar cell performance was related to the doping concentrations of NiO and PCBM, and the thicknesses of perovskite and NiO interlayer. The optimized performance of perovskite solar cells with power conversion efficiency (PCE) of 22.0% was achieved when doping concentrations of NiO and PCBM were $1 \times 10^{17} \text{ cm}^{-3}$ and $1 \times 10^{19} \text{ cm}^{-3}$, respectively, and thicknesses of perovskite and NiO were 450 nm and 30 nm, respectively. Moreover, a high PCE of 18.0% was obtained based on experimental condition. These results showed that this kind of solar cell was a potential choice for perovskite solar cells with high efficiency.

1. Introduction

In 2009, Miyasaka and co-workers employed $\text{CH}_3\text{NH}_3\text{PbI}_3$ and $\text{CH}_3\text{NH}_3\text{PbBr}_3$ as absorbers into solar cells, and power conversion efficiencies (PCEs) of 3.81% and 3.13% were obtained, respectively (Kojima et al., 2009). Since then, lots of works have been done to optimize the perovskite solar cell (PSC) performance. Different kinds of PSC structures have been studied during the past few years, such as perovskite sensitized solar cell (Burschka et al., 2013; Im et al., 2011; Kojima et al., 2009), mesoporous structured PSC (Kim et al., 2012; Lee et al., 2012; Wang et al., 2015), and planar heterojunction PSC (Jeon et al., 2015; Liu et al., 2013; Zhou et al., 2014). The simplest structure was planar heterojunction PSC due to the avoidance of high-temperature processed mesoporous layers (Jung and Park, 2015). The planar PSC does not contain mesoporous layers compared with the mesoporous structured PSC, thus the fabrication process is much simpler. Meanwhile, tandem solar cells could be achieved with planar PSCs and silicon or CIGS solar cells, and the device performance could be further improved (Bailie et al., 2015; McMeekin et al., 2016). Thus planar PSCs have attracted more and more attention. There are two kinds of planar PSCs: normal structure and inverted structure. The typical cell of normal structure is $\text{TCO}/\text{TiO}_2/\text{CH}_3\text{NH}_3\text{PbI}_3/\text{spiro-OMeTAD}/\text{Metal}$. In

Yang's report, PCE of 19.42% with active area of 0.1134 cm^2 has been realized (Yang et al., 2016). In Jiang's report, PCE of 19.9% with active area of 0.0737 cm^2 has been realized (Jiang et al., 2016). Both results mentioned above have been certified. For uncertified record, power conversion efficiency has achieved 20.0% (Momblona et al., 2016). Inverted planar heterojunction PSCs with p-i-n structure have drawn much attention as well. This kind of PSC could be fabricated by a low-temperature solution route (Chang et al., 2016b, 2016c; Docampo et al., 2013) and has less current hysteresis (Chang et al., 2016a; Sun et al., 2016; Xu et al., 2015). In Wu's report, a certified PCE of 18.21% with active area of 1.022 cm^2 has been realized (Wu et al., 2016). For uncertified record, power conversion efficiency has also achieved 20.0% (Bai et al., 2016). For future large area roll-to-roll fabrication, inverted structure is desirable due to its low temperature and simple fabrication process. In this study, we explored inverted planar PSCs. Because metal oxides demonstrated much higher carrier mobility and superior stability than organic materials (Hau et al., 2008; Qian et al., 2011), we employed nickel oxide (NiO) as the hole transport layer. Fan et al. found that using $\text{CH}_3\text{NH}_3\text{PbI}_{3-x}\text{Cl}_x$ as absorbers in PSCs could improve device performance with negligible photocurrent hysteresis because of better surface coverage (Fan et al., 2015). Moreover, $\text{CH}_3\text{NH}_3\text{PbI}_{3-x}\text{Cl}_x$ has advantages of facile high-quality film deposition and excellent

* Corresponding authors.

E-mail addresses: zhlin@xidian.edu.cn (Z. Lin), cfzhang@xidian.edu.cn (C. Zhang), jjingchang@xidian.edu.cn (J. Chang).

photovoltaic properties, and the diffusion length of $\text{CH}_3\text{NH}_3\text{PbI}_{3-x}\text{Cl}_x$ can exceed $1\ \mu\text{m}$ (Conings et al., 2014; Docampo et al., 2014; Eperon et al., 2014; Lee et al., 2012; Mauro, 2011; Stranks et al., 2013). The $\text{CH}_3\text{NH}_3\text{PbI}_{3-x}\text{Cl}_x$ solar cells exhibit high open circuit voltage (V_{oc}) ($\sim 1.1\ \text{V}$), and the qV_{oc}/E_{gap} value could reach up to 0.71 (Edri et al., 2014), where q is the electron charge and E_{gap} is the optical bandgap. Hence, we employed $\text{CH}_3\text{NH}_3\text{PbI}_{3-x}\text{Cl}_x$ as absorber. In this study, the structure of ITO/NiO/ $\text{CH}_3\text{NH}_3\text{PbI}_{3-x}\text{Cl}_x$ /PCBM/Ag was explored. The effects of the thicknesses of perovskite and NiO layers, and the doping concentrations of NiO and PCBM layers on PSC device performance were investigated. Under optimally simulative condition, a high PCE of 22% was achieved. Moreover, under the experimental condition, a high PCE of 18% could be successfully obtained, indicating that our work provided some guidance for the planar structure high performance perovskite solar cell.

2. Simulation and experiment

2.1. Simulation part

The simulation was mainly based on three basic equations which were Poisson's equation, carrier continuity equation and drift-diffusion equation:

$$\text{poisson's equation: } \frac{\partial^2 \varphi}{\partial x^2} = \frac{q}{\varepsilon}(n-p), \quad (1)$$

$$\text{carrier continuity equation: } \frac{\partial n}{\partial t} = \frac{1}{q} \frac{\partial J_n}{\partial x} + G - R, \quad \frac{\partial p}{\partial t} = -\frac{1}{q} \frac{\partial J_p}{\partial x} + G - R \quad (2)$$

$$J_n = qD_n \frac{\partial n}{\partial x} - q\mu_n n \frac{\partial \varphi}{\partial x}, \quad J_p = -qD_p \frac{\partial p}{\partial x} - q\mu_p p \frac{\partial \varphi}{\partial x}, \quad (3)$$

where φ is electric potential, ε is dielectric constant, q is electron charge, n is electron concentration, p is hole concentration, J_n is electron current density, J_p is hole current density, G is carriers generation rate, R is carriers recombination rate, D_n is electron diffusion coefficient, D_p is hole diffusion coefficient, μ_n is electron mobility, and μ_p is hole mobility.

Inverted planar structure ITO/NiO/ $\text{CH}_3\text{NH}_3\text{PbI}_{3-x}\text{Cl}_x$ /PCBM/Ag was used in the simulation, as shown in Fig. 1. ITO was applied as front contact for inverted planar PSCs, P-type doped NiO was employed as the hole transport layer, intrinsic $\text{CH}_3\text{NH}_3\text{PbI}_{3-x}\text{Cl}_x$ was used as absorber layer, N-type doping PCBM acted as electron transport layer, and Ag was used as metal rear contact. In the simulation, transfer-matrix method was used as optical model to calculate carrier generation rate. Shockley-Read-Hall (SRH) recombination, band to band recombination,

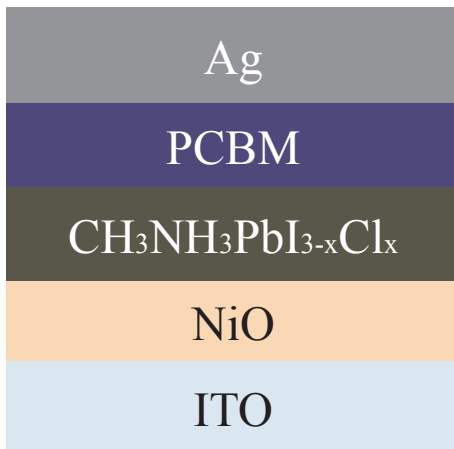


Fig. 1. Device structure used in the simulation.

Table 1

Simulation parameters of the perovskite solar cell, where ε_r was dielectric constant, E_g was bandgap, λ was electron affinity, N_c was effective conduction band density, N_v was effective valence band density, μ_n was electron mobility, and μ_p was hole mobility.

Parameter	NiO	$\text{CH}_3\text{NH}_3\text{PbI}_{3-x}\text{Cl}_x$	PCBM
Thickness (nm)	40	300	55
N_A (cm^{-3})	1×10^{16}	–	–
N_D (cm^{-3})	–	–	1×10^{17}
ε_r	11.75	6.5	4
E_g (eV)	3.6	1.55	2
λ (eV)	2.1	3.93	3.9
N_c (cm^{-3})	2.5×10^{20}	2.5×10^{20}	1×10^{21}
N_v (cm^{-3})	2.5×10^{20}	2.5×10^{20}	2×10^{20}
μ_n (cm^2/Vs)	0.001	2	0.01
μ_p (cm^2/Vs)	0.001	2	0.01

and Auger recombination were considered. The standard AM 1.5G solar spectrum was used to get current density-voltage (J - V) curve under illumination (Pandey et al., 2016). Material parameters of each layer were obtained from literatures and summarized in Table 1 (Hu et al., 2014; Malinkiewicz et al., 2013; Minemoto and Murata, 2016; Tsai et al., 2016; Shan et al., 2013).

2.2. Experimental part

For the solution processed NiO, 270.79 mg $\text{Ni}(\text{NO}_3)_2 \cdot 6\text{H}_2\text{O}$ (1.0 mmol) was dissolved in 2-methoxyethanol (10 ml). After the solution was stirred at $50\ ^\circ\text{C}$ for 1 h, $10\ \mu\text{l}$ acetylacetone was added to the solution, and then the solution was further stirred overnight at room temperature.

Planar PSCs were fabricated on pre-patterned fluorine tin oxide (FTO) or ITO glass substrates (around $2 \times 2.5\ \text{cm}^2$ in size, $10\ \Omega$ per square). The patterned ITO glass substrates were sequentially ultrasonic cleaned with detergent, de-ionized water, acetone, and isopropyl alcohol (IPA) at $50\ ^\circ\text{C}$ for 20 min, respectively. Then the ITO substrates were dried with nitrogen and treated in a UV ozone oven for 15 min. A thin layer of NiO was spin-coated on the substrates at 3000 rpm for 45 s and annealed at $250\ ^\circ\text{C}$ for 1 h. After that, the substrates were transferred into a nitrogen-filled glove box. $1.36\ \text{M}$ PbI_2 and $0.24\ \text{M}$ PbCl_2 were dissolved in the solvent of Dimethylformamide (DMF) and stirred for 2 h at $75\ ^\circ\text{C}$. $70\ \text{mg}$ methylammonium iodide (MAI) and $30\ \text{mg}$ formamidinium iodide (FAI) were dissolved in the solvent of IPA with $0.9\ \text{vol}\%$ DMF. Around $60\ \mu\text{l}$ PbX_2 precursor pre-heated to $75\ ^\circ\text{C}$ was transferred by pipettes to the NiO covered ITO substrates. Briefly, the spin coating process was programmed to run at 3000 rpm for 45 s. Then MAI was spin-coated on top of the dried PbI_2 layer at room temperature at 3000 rpm for 45 s. All of the films were thermally annealed on the hotplate at $100\ ^\circ\text{C}$ for 10 min. Next, a layer of PCBM (20 mg/ml in chlorobenzene) was spin-coated on the top of the perovskite layer at 2000 rpm for 40 s. The devices were finished by thermally evaporated $100\ \text{nm}$ Ag. All the devices had an effective area of $7.5\ \text{mm}^2$ defined by a shadow mask.

Photovoltaic performance was measured by using a Keithley 2400 source meter under simulated sunlight from XES-70S1 solar simulator matching the AM 1.5G standard with an intensity of $100\ \text{mW}/\text{cm}^2$. The system was calibrated against a NREL certified silicon reference solar cell.

3. Result and discussion

3.1. Influence of doping concentration of NiO layer

Energy band and recombination rate are related to the doping concentration of NiO. Therefore, acceptor doping concentration of NiO has considerable influence on the performance of perovskite solar cells.

Download English Version:

<https://daneshyari.com/en/article/7935129>

Download Persian Version:

<https://daneshyari.com/article/7935129>

[Daneshyari.com](https://daneshyari.com)